

The distance dependences and spatial uniformities of spectral irradiance standard lamps

Howard W. Yoon^{*a}, Gary D. Graham^b, Robert D. Saunders^a, Yuqin Zong^a, Eric L. Shirley^a

^aSensor Science Division, NIST, 100 Bureau Drive, Gaithersburg, MD 20899

^bITT Geospatial Systems Division, LLC, Rochester, New York 14606-0488

ABSTRACT

We describe the characterization of a group of NIST spectral irradiance lamps at longer distances and larger angles than are typically issued by NIST. The spectral irradiances from the FEL lamps were measured from 50 cm to 150 cm at 8 different distances using a cosine-corrected filter radiometer to determine if the lamps adhere to the inverse square law. Using the filter radiometer, the spatial uniformities of the FEL lamps were also mapped over a 20 cm square area at 135 cm, 143 cm and 151 cm. In the NIST goni-spectroradiometer facility, selected lamps were also mapped for the angular dependences of the spectral irradiances at a distance of 123 cm using a spectrograph which measures from 300 nm to 1100 nm for comparisons to the filter radiometer measurements. Using these measurements, an uncertainty budget for the distance and the angular uniformity correction of the FEL lamps was developed.

Keywords: spectral irradiance, NIST calibrated lamps, distance dependence

1. INTRODUCTION

The 1000 W FEL lamps issued by NIST and other national measurement institutes as standards of spectral irradiances are calibrated at a set distance and angular extent from a reference plane. NIST calibrates the FEL lamp using a spectroradiometer with a circular entrance aperture area of 1 cm^2 at a perpendicular distance of 50 cm from a reference plane. These spectral irradiance lamps are then often used in conjunction with reflectance panels to obtain spectral radiances to calibrate large field-of-view remote sensing sensors. These optical sensors which view large area targets should be calibrated using sources which are physically large enough to fill the field-of-view of the sensor. However, the calibration standards are often only calibrated over a limited range of physical parameters and must be characterized if they are to be used outside the calibrated settings.

We describe the use of a cosine-corrected filter radiometer to determine the distance corrections and the spatial uniformities of the spectral irradiances for a set of three FEL lamps. The angular responsivity of the filter radiometer was initially measured to determine whether the filter radiometer could be used for the FEL mapping and distance corrections using the inverse square law. The filter radiometer was also used to map the angular output of the FEL lamps at three different distances. The angular maps were also compared to those found using a goni-spectroradiometer at a distance of 123 cm. An uncertainty table has been developed for the use of the FEL lamps at the angles and distances outside the parameters used for the NIST calibration services.

2. EXPERIMENTAL SETUP

2.1 Gonio-filter radiometer (GOFR)

FEL lamps were measured using the gonio filter radiometer (GOFR) which is a cosine-response-corrected, filter radiometer whose spectral responsivity is centered at 648 nm. A schematic of the GOFR is shown in Fig. 1. The field-of-view (FOV) restrictor was used to reduce the signal from the stray radiation in the room. The flashed opal diffuser, interference filter and silicon photodiode are all aligned on the optical axis for optimal rotational symmetry of the angular responsivity. For temperature stability, the spectral filter and the diode are placed in a thermo-electric cooled copper block which is held near room temperature. A constant temperature is maintained during the calibrations to ensure for long-term stability of the GOFR responsivity. To achieve low-noise measurements, the photocurrent from the

^{*}howard.yoon@nist.gov; phone 1 301 975 2482; fax 1 301 869 5700

photodiode is directly amplified using a trans-impedance amplifier which is connected to the diode which are both shielded in a cylindrical mount. The preamplifier gains can be selected using a switch.

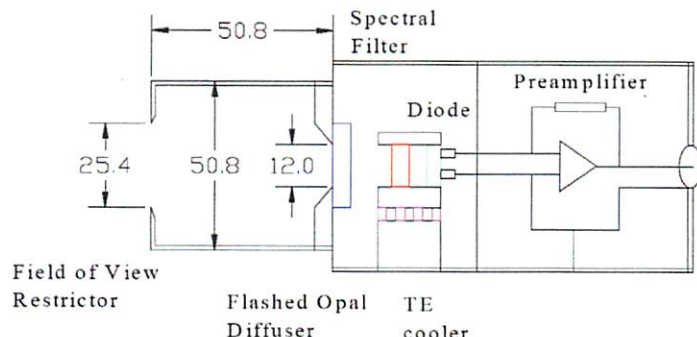


Figure 1. Schematic diagram of the GOFR. The dimensions are given in units of mm. The FOV restrictor was removed for the angular responsivity measurements.

2.2 Spectral responsivity of the GOFR

The GOFR's relative spectral response in a linear scale is shown in Fig. 2. The spectral responsivity of the GOFR was measured using a prism-grating double monochromator with a tungsten-ribbon filament source. The spectral power output of the monochromator was calibrated using a NIST-calibrated Si diode. The radiation was focused onto the flashed opal diffuser to fill the optics to reproduce the setup in the actual use of the GOFR. Its spectral responsivity is centered at 648 nm with a FWHM of about 15 nm. The wavelength of the interference filter was chosen to coincide with the previous angular screening of the FEL lamps performed at 655 nm. The lack of sharp rise and cutoff edges in the spectral responsivity could be attributed to the use of the diffuser.

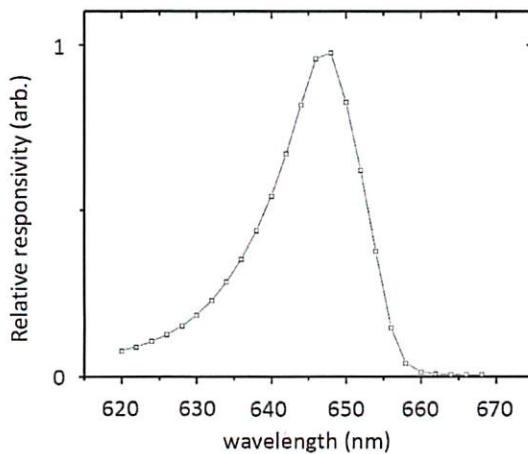


Figure 2. Relative spectral responsivity of the GOFR determined using a double monochromator.

2.3 Angular responsivity of the GOFR

Since the GOFR is used to measure the projected spectral irradiances in a plane, the cosine response of the radiometer must be determined. The cosine response of the GOFR was measured by mounting the radiometer on a goniometric rotation stage on a photometric bench and measuring its output signal as a voltage versus scan angle. The front surface

of the flashed opal diffuser was aligned to the center of the goniometric stage. This measurement was performed twice, once with the radiometer upright for horizontal cosine response, and once with the radiometer rotated by 90° for vertical cosine response. The data were then compared to a perfect cosine response and the percent differences from the perfect cosine response are plotted in Fig. 3. The deviations from a cosine angular response are due to the GOFR design with the use of the flashed opal, the interference filters and the Si diode. The radiation is being lost as the angle is changed from normal incidence, but the residuals from the fit are < 0.01 % over the ± 5 deg rotation angle in the horizontal and vertical directions.

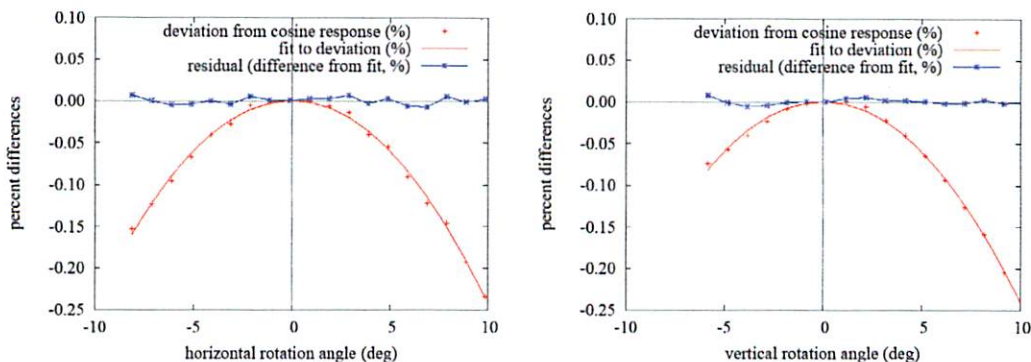


Figure 3. Percent difference of the GOFR response from perfect cosine response.

2.4 Motorized positioning

After the angular responsivity of the GOFR has been characterized, the GOFR was attached to motorized x, y and z stages for the distance and the x- and y-axis mapping measurements. The angular orientation of the GOFR was not changed for these measurements. An optical bench was used to ensure good optical alignment of the lamp with respect to the GOFR and its translation stage assembly. The position of the GOFR was varied so that it viewed the lamp from a variety of distances along the optical (z) axis during “z scans”, and at a range of (x,y) positions in constant-z planes, for the largest three values of z, during “x-y scans”. The stages are moved using ball screws attached to DC servo motors whose rotation is monitored using relative angular encoders with 2000 pulses per revolution. As stated by the stages’ manufacturer, the stages are capable of repeatability of ±1 µm with an accuracy of ±20 µm. Two of these stages were used for the z axis, in a configuration with one stage with a short range of travel being mounted on a second stage with a longer range of travel. This configuration was needed to achieve the required range of travel along z. Two other motorized stages were used for the positioning along x, and along y. A computer program was written to control all the axes and the data acquisition from the GOFR using a digital voltmeter.

2.5 Lamp current control

The FELs were mounted on a standard kinematic mount. The alignment jig was placed in the mount, and the optical axis was determined using a laser that was retroreflected from the jig. The lamp current was computer-controlled and periodically monitored from the voltage measurements using a calibrated shunt resistor in series with the lamp.

The uncertainty in lamp current is estimated to be <1.3 mA at the operational current of 8.2 A based on observed temporal variation (see Fig. 4). Published results for the UV/visible spectral range state the relative uncertainty in spectral irradiance as

$$\frac{u(E(\lambda))}{E(\lambda)} = 0.0006 \left(\frac{654.6 \text{ nm}}{\lambda} \right) u(I), \quad (1)$$

with $u(I)$ in mA (Eqn. D.9 in [1]).

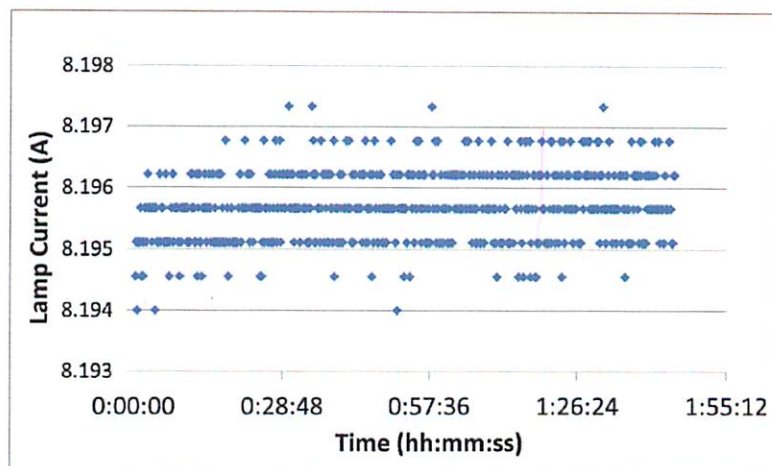


Figure 4. Temporal variation in measured lamp current. The standard deviation was determined from these results. The digitization of the results is due to the lack of sufficient resolution of the readout program.

2.6 Scattered light control

Baffles were used to suppress the scattered light. Varying the placement and number of baffles ensured that the ambient radiation was at greatest $\sim 0.1\%$ of the net signal. Thus any change in the location of scattering objects would lead to a small change in the net signals. Because the room could not be made completely dark, a field-of-view (FOV) restrictor was mounted in the front of the GOFR for ambient signal subtraction. Subtracting ambient signal with a direct-beam block during x-y and z scans compensated for remaining scattered-light effects. To compensate for the changing field-of-view as the z distance increased, a larger diameter direct-beam block was used at the larger distances.

3. FEL DISTANCE DEPENDENCE

The distances (synonymous with z positions in this paper) are measured from the plane tangent to the front of the FEL bi-posts and a plane at the front surface of the radiometer housing with the FOV restrictor removed. A calibrated internal micrometer was used to determine the measured distances as listed in Table 1. The front surface of the flashed opal diffuser was recessed from the radiometer front surface by $4.25\text{mm} \pm 0.05\text{mm}$, and the high-quality cosine response suggests that the flashed opal front surface is very close to the effective detector plane because of its nearly Lambertian character. Measurements were performed at 8 different z distances. Nominal and measured values of z distances and the ambient baffle diameters used at the respective distances are listed in Table 1.

Table 1. Nominal and measured z distances and baffle block diameters.

Nominal distance (cm)	Measured distance (cm)	Baffle Block Diameter (cm)
50	50.0510	2.54
61	60.9149	2.54
79	78.7720	7.5
97	96.5429	7.5
116	115.5913	10.0
135	134.6078	10.0
143	142.5635	10.0
151	150.8247	10.0

The measured distances along with the net signals at those distances were used to fit to Eq. 2 using a least-squares fit to minimize the residuals. Fig. 5 shows the residuals for the best fit of radiometer signal vs. z distance according to the fit equation,

$$S = a/(z+b)^2, \quad (2)$$

where a and b are fitting parameters.

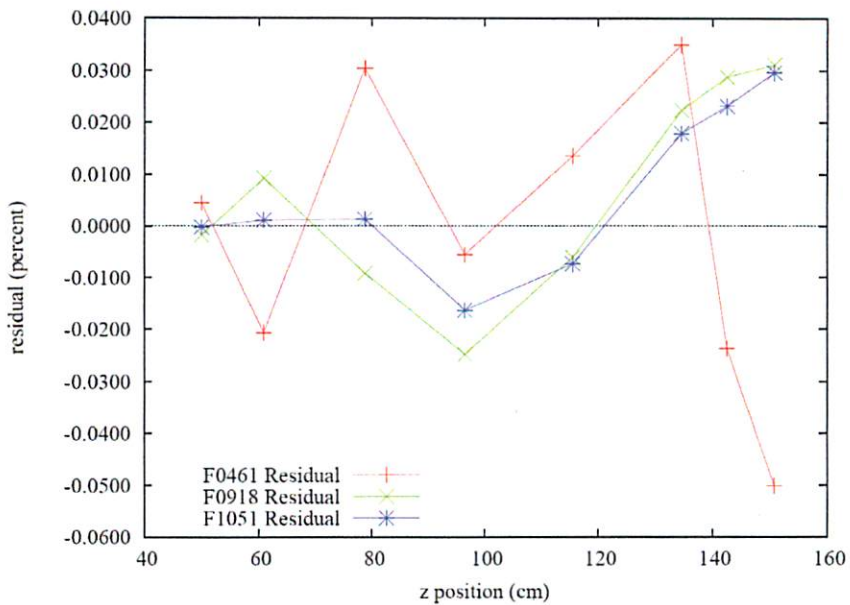


Figure 5. Residuals from fitting to form, $S = a/(z+b)^2$ for the three lamps. Note that two lamps show similar pattern to the residuals.

The best-fit values of a and b are shown in Table 2.

Table 2. Best-fit values of a and b parameters for FEL lamps under test.

Lamp	a (V cm^2)	b (mm)
F-461	17321.62	6.0906
F-918	17045.37	6.4367
F-1051	17715.34	6.9152

An offset distance can be estimated from the addition of the offset distance and the radius of the lamp posts. The b values are smaller than the estimate,

$$4.25 \text{ mm} + 3.175 \text{ mm} = 7.425 \text{ mm}, \quad (3)$$

which one might expect based on the actual distance between the lamp filament center and the flashed opal front surface. One can conjecture that this difference from 7.425 mm results from the apparent optical center of the lamps viewed from such z distances as being displaced slightly toward the detector, which views the near side of the filament more than the far side of the filament.

4. FEL ANGULAR DEPENDENCE

4.1 Spatial dependence of raw signals

The x-y scans were performed at three z distances corresponding to the nominal values of 135 cm, 143 cm and 151 cm. These measurements were performed immediately after the z-distance dependence measurements with the lamp continuously operating between these set of measurements. During the x-y scans, the detector position was varied in 12.7 mm steps along x and y to a total range of ± 8.89 cm along x or y, leading to 225 sampling positions in the nominal 143 cm, 151 cm and 135 cm planes in that respective sequence. The initial distance was set to 143 cm and the direct-beam block measurements were performed at the 225 positions. These ambient measurements were performed only at the 143 cm position using the 10 cm diameter direct-beam block and were used to subtract from the total signals at the other two positions to obtain the net signals. It was determined that the small changes in the z distance did not result in relevant differences in the ambient radiation. The results of the x-y scans are illustrated in Fig. 6 by the percent difference from unity of $S(x, y, z) / S(0, 0, z)$.

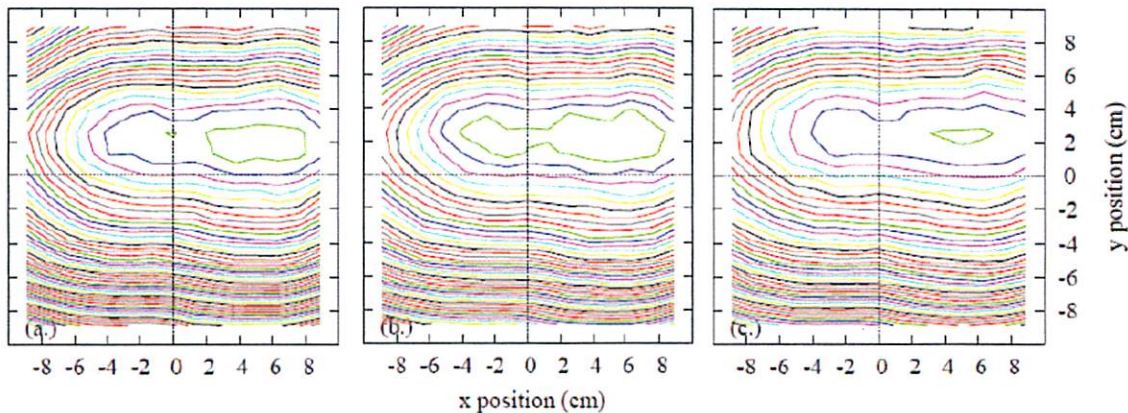


Fig. 6a-6c. $100\% \times [S(x, y, z) / S(0, 0, z) - 1]$ for lamp F-461 at nominal distances 135 cm, 143 cm and 151 cm. Contour intervals are 0.1 %; zero contour passes through the origin.

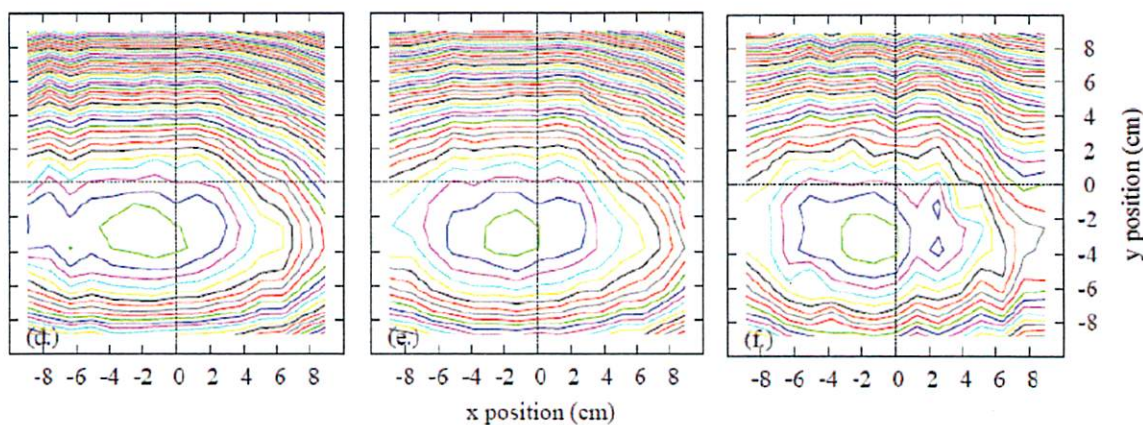


Fig. 6d-6f. $100\% \times [S(x, y, z) / S(0, 0, z) - 1]$ for lamp F-918 at nominal distances 135 cm, 143 cm and 151 cm. Contour intervals are 0.1 %; zero contour passes through the origin.

Return to the Manage Active Submissions page at <http://spie.org/app/submissions/tasks.aspx> and approve or disapprove this submission. Your manuscript will not be published without this approval. Please contact author_help@spie.org with any questions or concerns.

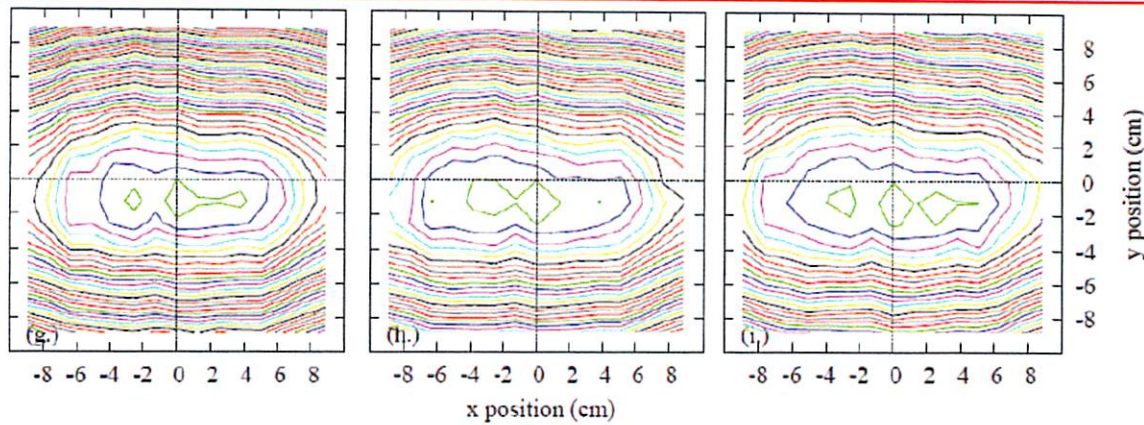


Fig. 6g-6i. $100\% \times [S(x, y, z) / S(0, 0, z) - 1]$ for lamp F-1051 at nominal distances 135 cm, 143 cm and 151 cm. Contour intervals are 0.1 %; zero contour passes through the origin.

The three different lamps have quite substantial differences in the angular projections at the three different distances. These differences arise from the fact that the filaments of the lamps are not aligned with the quartz envelopes or the lamp posts. Since the orientation of the filament to the outside envelope is set during the fabrication of the lamps, it is impossible to account for the variations in the coincidence of the optical axis with the physical axis.

4.2 FEL Angular dependence corrected for tilt of the GOFR

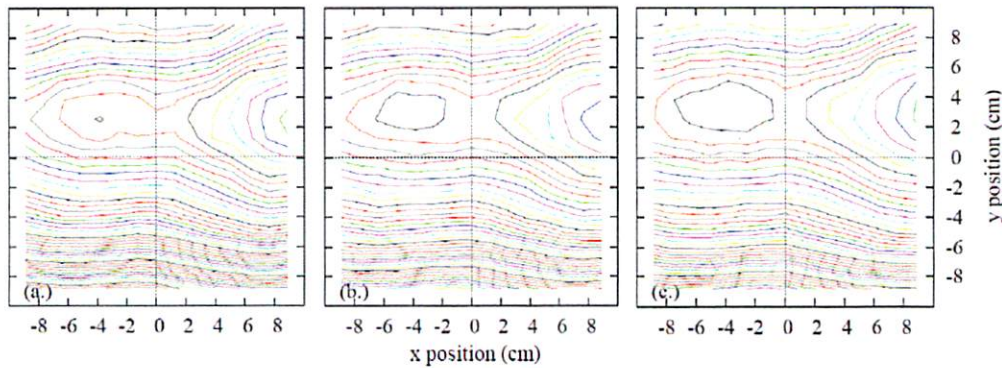
Throughout this report and in all materials that accompany it, the quantity $S(x, y, z)$ is proportional to the raw GOFR signal corrected for ambient subtraction and for the deviation of the GOFR from perfect cosine response as shown in Fig. 7. As an illustration, if instead of the FEL, an ideal point source could be located at distance $z + b$ from the GOFR effective detector area, then the quantity $R(x, y, z)$ in Eq. (4) would essentially be independent of the radiometer x and y position.

The raw irradiance signals can be corrected to obtain angular radiant intensity by using

$$R(x, y, z) = \left(\frac{S(x, y, z)}{S(0, 0, z)} \right) \left(\frac{x^2 + y^2 + (z + b)^2}{(z + b)^2} \right) / \cos \theta'. \quad (4)$$

Here, we have

$$\theta' = \cos^{-1} \left(\frac{z + b}{[x^2 + y^2 + (z + b)^2]^{1/2}} \right). \quad (5)$$



Please verify that (1) all pages are present, (2) all figures are correct, (3) all fonts and special characters are correct, and (4) all text and figures fit within the red margin lines shown on this review document. Complete formatting information is available at <http://SPIE.org/manuscripts>

Return to the Manage Active Submissions page at <http://spie.org/app/submissions/tasks.aspx> and approve or disapprove this submission. Your manuscript will not be published without this approval. Please contact author_help@spie.org with any questions or concerns.

Fig. 7a-7c. $100\% \times \{S(x, y, z)[x^2 + y^2 + (z + b)^2] \sec \theta' / [S(0, 0, z)(z + b)^2]\}$ for lamp F-461 at nominal distances 135 cm, 143 cm and 151 cm. Contour intervals are 0.1 %; zero contour passes through origin.

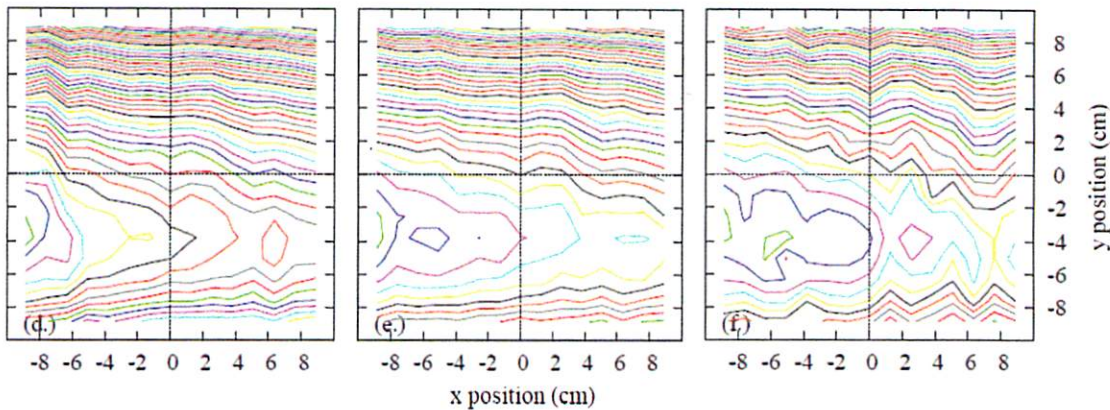


Fig. 7d-7f. $100\% \times \{S(x, y, z)[x^2 + y^2 + (z + b)^2] \sec \theta' / [S(0, 0, z)(z + b)^2]\}$ for lamp F-918 at nominal distances 135 cm, 143 cm and 151 cm. Contour intervals are 0.1 %; zero contour passes through origin.

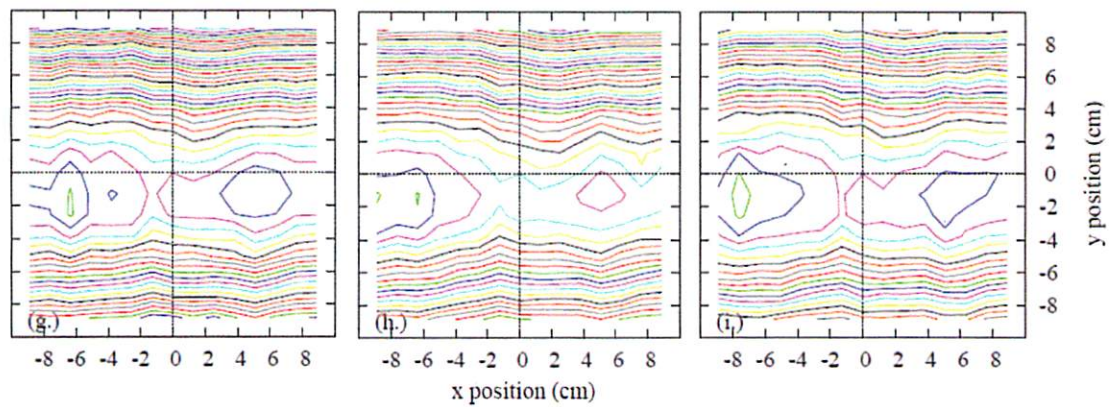


Fig. 7g-7i. $100\% \times \{S(x, y, z)[x^2 + y^2 + (z + b)^2] \sec \theta' / [S(0, 0, z)(z + b)^2]\}$ for lamp F-1051 at nominal distances 135 cm, 143 cm and 151 cm. Contour intervals are 0.1 %; zero contour passes through origin.

The smaller panel-to-panel variation shown in the latter plots confirms that, at such distances, radiometric intensity is essentially conserved if one conceives of the lamp as a fictitious point source, and that the radiometer does indeed have an ideal cosine response. The differences between the measurements at the respective distances compare well within less than 0.1 %. On the other hand, the asymmetry of Figs. 6-7 is attributed to filament tilt in the FELs.

4.3 Validation of the GOFR measurements using the NIST gonio-spectroradiometer facility

The angular distribution of spectral intensity emitted by several NIST-owned FELs was independently measured in the NIST gonio-spectroradiometer facility (GSF) in order to determine if there was an additional angular dependence of the FEL spectral irradiance which could not be measured using a single band filter radiometer such as the GOFR. In those tests, the radiant flux incident on a detector head was fed through a fiber to a spectroradiometer with the FEL at a

distance of about 123 cm from the entrance plane of the detector head [2]. The FEL was mounted on a rotating stage, which allowed for measurement of the variation of intensity with yaw angle with respect to the FEL front, in approximate analogy to scanning along x during the x-y scans. Likewise, the detector head was on a goniometer arm with an up-down axis of rotation passing transversely through the lamp center, which allowed for measurement of the variation of intensity with pitch angle, in approximate analogy to scanning along y during the x-y scans. (This arrangement also prevented lamp tilt and any associated filament sag effects.)

The spectroradiometer had 1024 spectral channels with wavelengths varying from about 300 nm to about 1100 nm. The spectral irradiances were grouped into 20 separate spectral bins (corresponding to 51.2 nm spectral widths). Therefore, in addition to validating the methodology employed on the optical bench for measuring lamp irradiance uniformity using the GOFR, these measurements also determined the degree of spectral dependence of the angular dependence of the lamp's spectral intensity (measured in angle space in spherical polar coordinates such that the origin is at the lamp center). In this regard, one can consider a "shape function" with the form of the ratio, $I_\lambda(\theta, \phi; \lambda) / I_\lambda(0, 0; \lambda)$. This is the ratio of the spectral intensity along a given direction to the spectral intensity along a fixed direction with $\theta = \phi = 0$, which corresponds to the z direction on the optical bench setup. This shape function has a value of unity for $\theta = \phi = 0$ but differs from unity elsewhere.

4.4 Comparison of the data between the GOFR setup and the gonio-spectroradiometer facility (GSF)

The variation in intensity vs x and y direction cosine is shown for NIST FEL F-240 in Figs. 8. Fig. 8a show the percent difference from the on-axis value as measured in the gonio spectroradiometer facility. Fig. 8b show the same quantity, as derived from measurements on the optical bench based on an x-y scan in the nominal 143 cm plane. Fig. 9 show the difference between the two results. The root-mean-square different between the two methodologies was about 1800 ppm in the angle space contained within a 76.2 mm vertical by 152.4 mm horizontal area section of that plane, and about 3100 ppm in a larger 152.4 mm by 152.4 mm area.

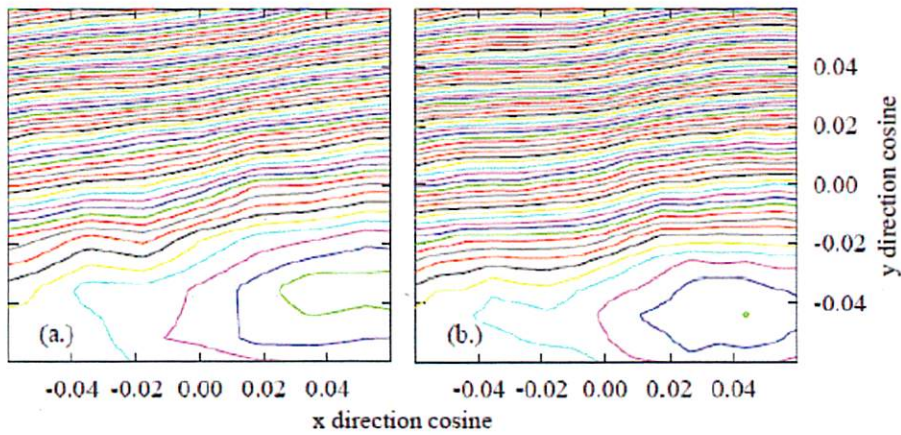


Figure 8. Intensity difference from center based for (a.) GSF measurements using GSF data for the bin closest to 647 nm, (b.) GOFR measurements

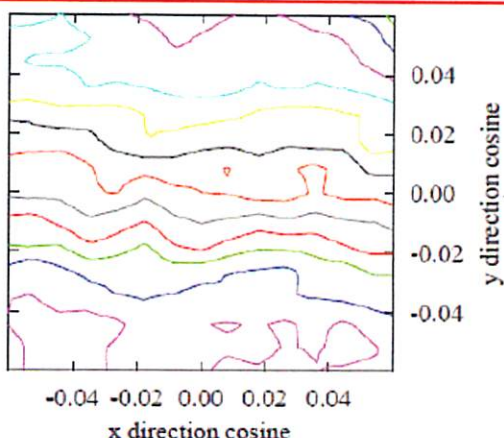


Figure 9. The GSF/GOFR differences. Results are plotted as contour plots vs direction cosines, with one contour per 0.1 % (1000 ppm) step and the zero contour passing through the origin.

4.5 Angular dependence of the spectral irradiances using the GSF

In order to determine whether the FEL lamp had any spectral variation with respect to the angular output, the 1024 spectral channels were band averaged into 20 separate spectral bins and then compared to the overall spectral irradiances. A roughly 768 ppm or 0.08 % r.m.s. differences in the binned shape functions were found as based on bin-to-bin comparisons as shown in Fig. 10. This small difference results from slight change of correlated color temperature (CCT)[3] with respect to the angle as shown in Fig. 11. This can be considered an uncertainty component for deduced uniformity of the spectral irradiances if the wavelength dependence of the shape function is neglected, and the GOFR results at a single centroid wavelength is otherwise assumed to be representative of spectral radiance in all spectral bands of interest. We expect that this same uncertainty would apply at wavelengths between 1100 nm and 2500 nm, because such wavelengths lie within the long-wavelength region of the Planck spectrum for a blackbody source most analogous to the FELs. In this region, the spectral radiance is less sensitive to filament temperature and lamp current fluctuations.

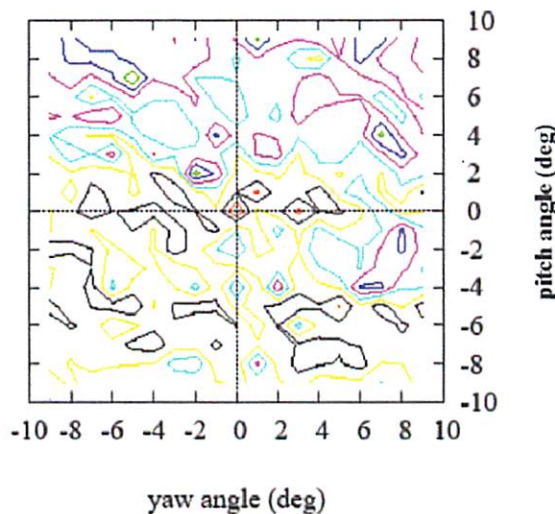


Figure 10. Root-mean-square variation of binned GSF results for 20 spectral bins as described in the text, versus direction. The binned shape functions were normalized to be equal to unity at the center, where the variation is by definition zero. Contours shown are 0.02 % (200 ppm) steps.

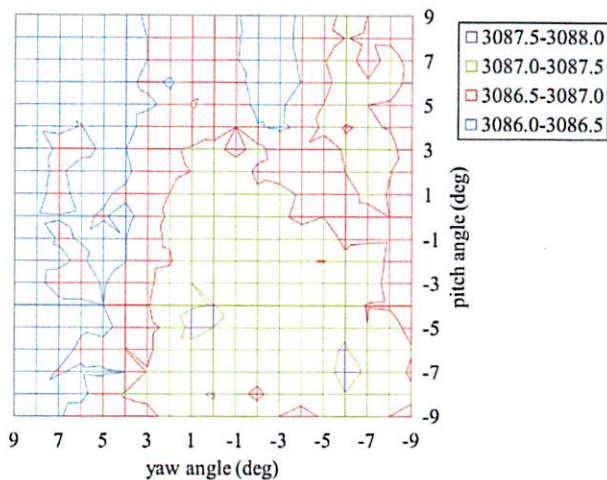


Figure 11. The correlated color temperature of the FEL lamp F-240 versus direction. Each contour denotes a change of 0.5 K. The differences are at most ± 1 K from the center value of 3087 K.

5. UNCERTAINTY BUDGET

The uncertainty budget for the GOFR spatial scans and the total uncertainties including the spectral-gonio dependence of the spectral irradiances are given in Table 3. The individual uncertainty components are obtained from the pertinent measurements. The distance uncertainties are estimated from the spread in the residuals from the fits in Fig. 5. The GOFR gono corrections are obtained from the residuals from the gono-corrected fit in Fig. 3. The lamp control uncertainties are estimated from the current setting limit of 1.3 mA converted to a spectral irradiance uncertainty. The scattered-light-control uncertainties are determined from various designs and configurations of baffles during the measurements. Uncertainties because of the GOFR signal-to-noise ratio and stability are determined using repeated measurements with the GOFR and from knowledge of the temperature stability of the filter and the detector. The position repeatability is estimated from the repeatability of the contours seen in Figs. 6a-6i and is reasonable in view of our ability to repeatedly set position of the motorized stages using encoder feedback servo motors.

Fig. 10 shows that the spatial uniformity of the spectral irradiance from the FEL can be measured using a single spectral band, because angular variations are independent of wavelength within our uncertainties as assessed from the mapping of the CCT shown in Fig. 11. These measurements are confirmed by measurements of two other FEL lamps. Since the measurement of the spectral-gonio dependence were performed in another facility using different lamps than the ones used for the GOFR measurements, this observation is assumed to hold for other FEL lamps. This is incorporated in Table 3 on the 8th line.

A second critical issue that is outside of the scope of the optical bench measurements is the fact that the data products in this report can be used to derive ratios of irradiances, whereas setting the absolute scale for irradiances requires that the FEL have been calibrated in a separate measurement, such as according to the NIST SP-250-89 [4]. Furthermore, because the data products are ratios, errors in the numerator and denominator of a ratio compound for items in Table 3 on the 3rd, 5th and 6th lines.

A third critical issue that is outside of the scope of the optical bench measurements is that additional uncertainty components may be incurred when one seeks to know irradiances at points at which they were not measured using interpolation methods.

Table 3. The uncertainty table for the spatial uniformity measurements.

Line	Uncertainty	Type	Value (%)	Sensitivity	Value (%)
1	Distance	A	0.03	2	0.06
2	GOFR Gonio Correction	A	0.01	1	0.01
3	Lamp control	A	0.11	1	0.11
4	Scattered light control	B	0.05	1	0.05
5	GOFR signal-to-noise and stability	A	0.0014	1	0.0014
6	Position repeatability	A	0.07	1	0.07
7	GOFR total (1 to 6) ($k=1$)				0.18
8	Spectral-Gonio Dependence	B	0.09	1	0.09
9	Total ($k=1$)				0.20
10	Expanded ($k=2$)				0.40

6. DISCUSSION

If the NIST-calibrated FEL lamps are used as spectral irradiance standards outside the angular extend of the calibrations, then the angular uniformity of the lamps should be mapped. Since there is no assurance that the optical axis coincides with the physical axis, the difference of the optical center from the physical center should be measured. The deviations from the physical center were found to be the greatest for the lamp F-461 with the greatest deviation of the optical axis from the physical axis as seen in Figs. 6a-6c. However, if the three measured lamps constitute a representative set of lamps, then the assumption of the physical axis to be the same as the optical axis would result in a ± 1 mm ($k=1$) uncertainty for the distance correction needed when the FEL lamps are used at distances other than the 50 cm calibrated setting. The correction for the optical center is shown in

$$E(z) = E(50\text{cm}) \frac{(50+b)^2}{(z+b)^2}, \quad (6)$$

where z is the distance where the spectral irradiances is calculated from the provided values at 50 cm. The correction to the optical center occurs as a ratio.

7. CONCLUSIONS

The spatial uniformities of the FEL spectral irradiance standards can be measured using a filter radiometer with a cosine-correcting diffuser. The goniometer filter radiometer was designed for long-term stability, low-noise signal output and characterized for the uniformity of the angular response. Although the GOFR can only measure the distance dependence and the spatial uniformity in a single, quasi-monochromatic spectral band, the additional measurements using the goniometer-radiometer facility demonstrated that the spectral shape of the irradiances from the FEL does not strongly depend on the angle. Thus the GOFR measurements can be used to determine the spectral irradiances at different distances, angles and wavelengths. The total expanded uncertainty of the angular uniformity correction is estimated to be 0.40 %

Please verify that (1) all pages are present, (2) all figures are correct, (3) all fonts and special characters are correct, and (4) all text and figures fit within the red margin lines shown on this review document. Complete formatting information is available at <http://SPIE.org/manuscripts>

Return to the Manage Active Submissions page at <http://spie.org/app/submissions/tasks.aspx> and approve or disapprove this submission. Your manuscript will not be published without this approval. Please contact author_help@spie.org with any questions or concerns.

($k=2$). The total uncertainty of the spectral irradiances at these positions must also include the stated absolute scale uncertainties, which are not included Table 3.

Due to the agreement between the GOFR-determined spatial uniformities and those determined using the goni-spectroradiometer facility in the central region agree to about 0.3 % or better, any future demand for similar measurements could be accommodated in the NIST goni-spectroradiometer facility.

REFERENCES

This document is not subject to the controls of the International Traffic in Arms Regulations (ITAR) or the Export Administration Regulations (EAR).

- [1] Early, E., et al., "The 1995 North American Interagency Intercomparison of Ultraviolet Monitoring Spectroradiometers," *J. Res. NIST* 103, 15-62 (1998).
- [2] Zong Y. and Ohno Y., Realization of total spectral radiant flux scale and calibration service at NIST, Proc. of the CIE 26th Session, Beijing, China, D2-179 (2007).
- [3] CIE Publication No. 17.4, CIE International Lighting Vocabulary (1987).
- [4] Yoon, H.W. and Gibson, C.G., "Spectral Irradiance Calibrations," National Institute of Standards and Technology Special Publication 250-89 Nat. Inst. Stand. Technol. Spec. Publ. 250-89, 132 pp. (July 2011).